KURENAI
Kyoto University Research Information Repository

KYOTO UNIVERSITY

Title	Electrostatically constrained -helical peptide inhibits replication of HIV-1 resistant to enfuvirtide.
Author(s)	Nishikawa, Hiroki; Nakamura, Shota; Kodama, Eiichi; Ito, Saori; Kajiwara, Keiko; Izumi, Kazuki; Sakagami, Yasuko; Oishi, Shinya; Ohkubo, Tadayasu; Kobayashi, Yuji; Otaka, Akira; Fujii, Nobutaka; Matsuoka, Masao
Citation	The international journal of biochemistry & cell biology (2009), 41(4): 891-899
Issue Date	2009-04
URL	http://hdl.handle.net/2433/137209
Right	© 2009 Elsevier B.V.
Type	Journal Article
Textversion	author

Classification: Original article

ELECTROSTATICALLY CONSTRAINED α-HELICAL PEPTIDE INHIBITS REPLICATION OF HIV-1 RESISTANT TO ENFUVIRTIDE

Hiroki Nishikawa[1], Shota Nakamura[2], Eiichi Kodama[3]*, Saori Ito[1], Keiko Kajiwara[3,4], Kazuki Izumi[3], Yasuko Sakagami[3], Shinya Oishi[1], Tadayasu Ohkubo[5], Yuji Kobayashi[6], Akira Otaka[7], Nobutaka Fujii[1], Masao Matsuoka[3].

Graduate School of Pharmaceutical Sciences[1], Kyoto University, Sakyo-ku, Kyoto 606-8501, Japan, Research Institute for Microbial Diseases[2], Osaka University, Suita, Osaka 565-0871, Japan, Laboratory of Virus Control[3], Institute for Virus Research, and Graduate School of Biostudies[4], Kyoto University, Sakyo-ku, Kyoto 606-8507, Japan, Graduate School of Pharmaceutical Sciences[5], Osaka University, Suita, Osaka 565-0871, Japan, Osaka University of Pharmaceutical Sciences[6], Takatsuki, Osaka 569-1094, Japan, Graduate School of Pharmaceutical Sciences[7], The University of Tokushima, Tokushima 770-8505, Japan

Address correspondence to: Eiichi Kodama, MD, PhD, 53 Kawaramachi Shogoin, Sakyo-ku, Kyoto, 606-8507, E-mail: ekodama@virus.kyoto-u.ac.jp, Tel & Fax: +81-75-751-3986

1

Abstract

α-Helical peptides, such as T-20 (enfuvirtide) and C34, derived from the gp41 carboxyl terminal heptad repeat (C-HR) of HIV-1, inhibit membrane fusion of HIV-1 and the target cells. Although T-20 effectively suppresses the replication of multi-drug resistant HIV variants both in vitro and in vivo, prolonged therapy with T-20 induces emergence of T-20 resistant variants. In order to suppress the emergence of such resistant variants, we introduced charged and hydrophilic amino acids, glutamic acid (E) and lysine (K), at the solvent accessible site of C34. In particular, the modified peptide, SC34EK, demonstrates remarkably potent inhibition of membrane fusion by the resistant HIV-1 variants as well as wild type viruses. The activity was specific to HIV-1 and little influenced by serum components. We found a strong correlation between the anti-HIV-1 activities of these peptides and the thermostabilities of the 6-helix bundles that are formed with these peptides. We also obtained the crystal structure of SC34EK in complex with a 36 amino acid sequence (N36) comprising the amino terminal heptad repeat of HIV-1. The EK substitutions in the sequence of SC34EK were directed toward the solvent and generated an electrostatic potential, which may result in enhanced α-helicity of the peptide inhibitor. The 6-helix bundle complex of SC34EK with N36 appears to be structurally similar to that of C34 and N36. Our approach to enhancing α-helicity of the peptide inhibitor may enable future design of highly effective and specific HIV-1 inhibitors.

Key words; HIV; fusion; peptide; inhibitor; α-helix

1. Introduction

Enfuvirtide (T-20), which has been clinically approved as the first fusion inhibitor of HIV-1, is derived from a 36 amino acid region of the carboxyl-terminal heptad repeat (C-HR) of gp41, an HIV-1 transmembrane envelope glycoprotein, which plays central role in the fusion of HIV-1 with host cells.   T-20 prevents the formation of a 6-helix bundle, which is comprised of a trimer of dimers formed from the amino-terminal heptad repeat (N-HR) and the carbon-terminal heptad repeat (C-HR) in an antiparallel orientation.   Six helix formation by physiological gp41 enables host cell and virus membranes to contact and fuse, enabling the virus entry into the cells.   Therefore, inhibition of the formation of this 6-helix bundle prevents fusion of HIV-1 and targeted host cell membranes (Derdeyn et al., 2000; Wild et al., 1992). Notably, T-20 effectively suppresses the replication of HIV-1 variants, which are resistant to multiple reverse transcriptase and protease inhibitors, and has been used in the optimized regimens for HIV-1-infected patients harboring multi-drug resistant HIV-1 variants (Lalezari et al., 2003; Lazzarin et al., 2003).

Emergence of T-20-resistant HIV-1 was reported in patients receiving not only T-20 monotherapy in a phase I clinical trial (Wei et al., 2002), but also in patients treated with a combination of T-20 and other inhibitors in subsequent phase II and III trials (Matthews et al., 2004; Poveda et al., 2002).   These resistant variants frequently acquired mutations in gp41, especially in amino acids 36-45 of the N-HR region (Aquaro et al., 2006; Cabrera et al., 2006; Mink et al., 2005; Poveda et al., 2002; Rimsky et al., 1998; Wei et al., 2002) (**Fig. 1**).

Additionally, complementary mutations in the C-HR region, such as S138A mutation, were found in some T-20 resistant variants (Cabrera et al., 2006; Poveda et al., 2004; Xu et al., 2005). Introduction of these complementary mutations compensates for impaired HIV-1 replication stemming from the primary mutations that give rise to resistance. The N43D mutation in the N-HR region that confers resistance to T-20 is a well documented example (Xu et al., 2005).

Although T-20 inhibits gp41-mediated fusion (Derdeyn et al., 2000; Wild et al., 1992), it has additional effects on HIV-1 replication. For instance, baseline sensitivity of HIV-1 to T-20 is influenced not only by the amino acid sequence of gp41, but also by the co-receptor specificity (CCR5/CXCR4) defined by the structure of the V3 loop of gp120, a glycoprotein capping gp41, which binds to the CD4 cells (Derdeyn et al., 2000; Derdeyn et al., 2001). Moreover, substitutions within the CD4 binding domain of gp120 also contribute to the resistance of the virus to T-20 (Baldwin and Berkhout, 2006). Thus, the mode of action and the mechanism of resistance to T-20 seem to be complicated. In contrast, another fusion inhibitor known as C34, has been clearly shown to bind to the N-HR in vitro and act as a decoy of gp41 C-HR and prevent the formation of the 6 helix bundle (Chan et al., 1997; Liu et al., 2005; Xu et al., 2007) . Its inhibitory effect is over 10-fold greater than that of T-20 (Armand-Ugon et al., 2003; Nameki et al., 2005). Thus, C34 appears to be a suitable peptide to employ in the rational design of an improved HIV fusion inhibitor, based on the interaction between the peptide and the target.

It has been reported that α-helicity of the C-HR and N-HR peptide complexes correlates

with the anti-HIV-1 activity of the peptide inhibitor (Chan et al., 1998), suggesting that

enhancement of α-helicity of C34 may provide higher affinity to the N-HR region, thus

resulting in more potent anti-HIV-1 activity.   To design potent fusion inhibitors using the

enhancement of α-helicity approach, we divided the α-helical peptide C34 into two

characteristic interactive (*a, d, e*) and solvent accessible (*b, c, f, g*) sites according to the

reported N36/C34 structure (**Fig. 1**) (Chan et al., 1997).   When HIV-1 gp41 is folded, a

tryptophan-rich domain (WRD) in the N-terminus of C-HR plays an important role in tight and

specific binding, through the interaction of the hydrophobic aromatic ring with a deep groove

formed by the N-HR coiled coil (Chan and Kim, 1998; Salzwedel et al., 1999).   In fact, C34

contains the N-terminal WRD, which binds to a hydrophobic pocket formed by the amino acid

residues L57, W60 and K63 on the N-HR trimer surface (Chan et al., 1998; Ferrer et al., 1999),

resulting in higher anti-HIV-1 activity of C34 compared to T-20, which lacks the N-terminal

WRD.   On the other hand, the solvent accessible site appears to contribute little to the

formation of the 6-helix bundles, as demonstrated by the crystal structure of C34 bound to N36

(Chan et al., 1997).   Therefore, amino acids in the interactive site are indispensable for binding,

whereas those in the solvent accessible site may be replaceable (**Fig. 1**).   To enhance the

α-helicity of C34, we introduced a series of systematic replacements of amino acid residues in

the solvent accessible site, where the original amino acid residues were substituted with charged

and hydrophilic glutamic acid (E) or lysine (K) with the intention of forming possible

intrahelical salt-bridges (Marqusee and Baldwin, 1987) (**Fig. 1b**).   We obtained two peptides,

SC34 and SC34EK (**Fig. 2a**), which gratifyingly, both demonstrated increased anti-HIV-1

activity (Otaka et al., 2002).

In this study, we demonstrate that SC34EK maintains highly potent activity against T-20

resistant clones of HIV-1, as well as several clinical isolates, and we reveal that the enhanced

α-helicity of SC34EK is indeed involved in the improvement of activity.   The activities are

specific to HIV-1 and are not influenced by serum components.   Structural analysis indicates

that electrostatic interactions introduced by EK substitutions enhance the conformational

stability of the 6-helix bundle, thus preventing HIV-1 fusion with the host cell.   The

information from our investigations involving the enhanced α-helicity of SC34EK should

enable further design of highly effective and specific HIV-1 inhibitors.

2. Materials and Methods

2.1. Cells and Viruses

MT-2 and 293T cells were grown in RPMI1640- and Dulbecco's modified Eagle medium

(DMEM)-based culture medium, respectively.   HeLa-CD4-LTR-β-gal cells were kindly

provided by Dr. M. Emerman through the AIDS Research and Reference Reagent Program,

Division of AIDS, National Institute of Allergy and Infectious Disease (NIAID) (Bethesda, MD)

and were used for the drug susceptibility assay (MAGI assay) as described previously (Kimpton

and Emerman, 1992; Kodama et al., 2001; Maeda et al., 1998).   The activity of test compounds

was determined as the concentration that blocked HIV-1 replication by 50% (EC_{50}).

Laboratory HIV-1 (III$_B$) and HIV-2 (EHO and ROD) strains were used. An HIV-1

infectious clone pNL4-3 was used for constructions and for the production of HIV-1 variants as

described (Nameki et al., 2005). A wild type HIV-1, HIV-1$_{WT}$, was generated by transfection

of pNL4-3 into 293T cells. Clinical isolates obtained from drug-naïve and heavily

drug-experienced patients, were kindly provided by Dr. S. Oka (AIDS Clinical Center,

International Medical Center of Japan, Tokyo, Japan). Their co-receptor tropisms were

determined using NCK45 cells as described previously (Kajiwara et al., 2006).

2.2. Antiviral agent

The peptide-based fusion inhibitors used in this study were synthesized as described

previously (Otaka et al., 2002), and the sequences can be identified in **Fig. 2a**.

3′-Azido-3′-deoxythymidine (AZT) and 2,3′ -dideoxycytidine (ddC) were purchased from

Sigma (St. Louis, MO, USA). MKC-442 was provided by Dr. S. Shigeta (Fukushima Medical

University, Fukushima, Japan).

2.3. Determination of drug susceptibility of HIV-1

The peptide sensitivity of infectious clones was determined using the MAGI assay with as

described previously (Kodama et al., 2001; Maeda et al., 1998). The activity of test

compounds was determined as the concentration that blocks HIV-1 replication by 50% (EC$_{50}$).

For clinical isolates, PHA-stimulated peripheral blood mononuclear cells (PBMCs) were used

as described previously (Kodama et al., 2001). PBMCs (10^6 cells/ml) were exposed to test

compounds and HIV-1, and were cultured in the presence of interleukin 2 for 7 days. Amounts

of p24 protein in the supernatants of the cultures were then determined using the commercially available p24 antigen enzyme linked solvent assay kit.

2.4. Construction of recombinant HIV-1 clone

Recombinant infectious HIV-1 clones with substituted V3 regions, pNL-V3$_{ADA}$ and pNL-V3$_{SF162}$ were generated using pNL4-3.   The V3 region, corresponding to n.t. 7029 to 7249 of pNL4-3, was amplified using primers containing appropriate *Bgl* II and *Nhe* I restriction enzyme cleavage sites for directional cloning into pBS-gp120$_{WT}$.   The resulting amplified V3 region was subjected to *Bgl* II and *Nhe* I digestion, subcloned into pBS-gp120$_{WT}$ containing the corresponding region in the DNA fragment of *EcoR* I-*Nhe* I (1510 bp containing gp120 V1, V2 and V3, n.t. 5740 to 7249 of pNL4-3) and subsequently ligated into pNL4-3.   pNL-V3$_{CH1}$ and V3$_{CH2}$, CCR5 and dual (CXCR4 and CCR5) tropic molecular clones, were kindly donated by Dr. Y. Maeda, Kumamoto University (Kumamoto, Japan) (Foda et al., 2001; Maeda et al., 2000).

Recombinant infectious HIV-1 clones carrying various mutations in gp120 and/or gp41 were also generated using pNL4-3.   Briefly, the desired mutations were introduced using site directed mutagenesis into the region of pSL-gp41$_{WT}$ flanked by the *Nhe* I-*BamH* I restriction enzyme sites (1220 bp containing gp120 V4, V5 and gp41 ectodomain n.t. 7250 to 8469 of pNL4-3)(Weiner et al., 1994).   After restriction enzyme digestion and purification the *Nhe* I-*BamH* I fragments were ligated into pNL4-3, generating a series of molecular clones with the desired mutations.

Each molecular clone was transfected into 293T cells (10^5 cells/6-well culture plate).

After 48 h, MT-2 cells (10^6 cells/well) were added and co-cultured with the 293T cells for an additional 24 h. When an extensive cytopathic effect was observed, the supernatants were harvested and stored at -80˚C for further use.

2.5. Determination of gp41 amino acid sequence

Nucleotide sequences of the clinical isolates were determined using an automated sequencer. Briefly, DNA was extracted from PBMCs infected with the clinical isolates, subjected to nested PCR for the gp41 coding region, and then directly sequenced as described previously (Nameki et al., 2005).

2.6. Measurement of circular dichroism (CD) spectra

N-HR peptides (N36, N36$_{V38A}$ or N36$_{N43D}$) and C-HR peptides (C34 or SC34EK) were incubated at 37ºC for 30 min (the final concentration of both the N-HR peptide and the C-HR peptide were 10 μM in pH 7.4, 12 mM phosphate-buffered solution containing 50 mM NaCl). The wavelength-dependence of molar ellipticity [θ] was monitored at 25ºC as the average of eight scans, and the thermal stability was estimated by monitoring the change in the CD signal at 222 nm in a spectropolarimeter (Model J-710; Jasco, Tokyo, Japan) equipped with a thermoelectric temperature controller. The midpoint of thermal unfolding transition (melting temperature [T_m]) of each complex was determined as described previously (Otaka et al., 2002). The percentages of a-helicity in 6-helix complexes were calculated by comparing the CD signal at 222 nm of N36/C34 or N36/SC34EK complexes in a spectropolarimeter.

2.7. Crystallization, data collection and refinement

Samples for crystallization were prepared by mixing solutions of N36 and SC34EK

dissolved in 10 mM sodium acetate buffer at a concentration of 10 mg/mL.   The mixture was

incubated for 30 min at 37ºC, then was passed through a 22 μm filter.   Crystallization was

performed by the hanging drop vapor diffusion method at 4ºC.   Droplets were prepared of

equal amounts (2 μL) of reservoir solution and the peptide solution.   Hexagonal prism crystals

were obtained under the following conditions: 100 mM sodium acetate buffer (pH 4.0), 200 mM

ammonium sulphate, 14% polyethylene glycol monomethyl ether 2000.   After screening of

various cryo-conditions, the suitable condition was found to be the addition of 35% xylitol to

the peptide solution and a slight increase in the amount of the precipitant (*ca* 14.5%).   The

obtained crystals were easily broken by direct transfer from the crystallization condition to the

cryo-condition, but the transfer of the fragile crystals could be accomplished by gradual change

in conditions using stepwise increase in the amount (0 to 35% in five steps) of the

cryoprotectant.

Data was collected at a beamline BL38B1 of SPring-8.   Collected data were processed

using DENZO and SCALEPACK from the HKL2000 package (Otwinowski and Minor, 1997).

A molecular replacement solution was found using AMoRe (Navaza, 2001), with a molecular

model of the HIV-1 gp41 core structure (PDB code: 1AIK).   Model refinements and

reconstruction were performed using REFMAC5 (Murshudov et al., 1999) and XtalView

(McRee, 1999).   The final model was refined at a resolution of 2.1 Å, to a crystallographic *R*

value of 0.213 and a free *R* value of 0.238.   Detailed data collection and refinement statistics

are summarized in Table 1.　　Atomic coordinates and structural factors have been deposited at

the Protein Data Bank (**PDB code: 2Z2T**).

3. Results

3.1. Anti-HIV-1 activity of SC34 and SC34EK.

We examined the anti-HIV-1 activity of SC34 and SC34EK against not only HIV-1$_{WT}$ but

also T-20- and/or C34-resistant clones observed in vitro.　　SC34 and especially SC34EK that

has aligned EK modification more effectively suppress HIV-1 infection compared to C34 and

T-20 (**Table 1**).　　D36S/V38M substitutions in the gp41 region (HIV-1$_{D36S/V38M}$), and a five

amino acid (FNSTW) deletion in the V4 region of gp120 (ΔV4) with L33S/N43K in the gp41

region (HIV-1$_{ΔV4/L33S/N43K}$) were isolated in vitro (Fikkert et al., 2002; Rimsky et al., 1998).

L33S was also selected during C34-resistant induction in vitro (Armand-Ugon et al., 2003).

C34 and its derivatives effectively inhibit entry of these clones into the host cell.　　In particular,

SC34EK maintained strong activity even against V38E containing clones, such as HIV-1$_{V38E/N42S}$

(Armand-Ugon et al., 2003), which showed cross-resistance to T-20, C34 and SC34.

Reduction of activities by SC34 and SC34EK was moderate in HIV-1$_{ΔFNSTW/L33S/N43K}$ that

showed high level resistance to T-20 and C34.　　Next, we examined the antiviral activities of

C34 derivatives against clones containing major primary mutations V38A and N43D, which are

mutations frequently observed in T-20 resistant variants in vivo (Cabrera et al., 2006; Derdeyn

et al., 2001; Menzo et al., 2004; Poveda et al., 2004; Poveda et al., 2002; Xu et al., 2005) (**Table**

11

1).   SC34 reduced its antiviral activities against HIV-1$_{N43D}$, while SC34EK maintained its potent activity, indicating that when EK is bound with the complementary electrostatic interactions appropriately aligned SC34EK can effectively suppress the infection by various clones resistant to T-20 and C34 both in vitro and in vivo.

We further evaluated activities of SC34 and SC34EK against V3-substituted clones (**Table 1**).   HIV-1$_{V3-ADA}$ uses mainly the CCR5 co-receptor for its entry into the host cells and has been reported to moderate T-20 resistance ($\approx$10 fold), compared to the CXCR4 using strain of HIV-1, which shows higher susceptibility to fusion inhibitors (Reeves et al., 2002).   As reported, the susceptibility of HIV-1$_{V3-ADA}$ to T-20 decreased, however, C34 and its derivatives maintained their activity against the same variant.   Interestingly, in our experiments, HIV-1$_{V3-SF162}$, HIV-1$_{V3-CH1}$ and HIV-1$_{V3-CH2}$ also showed comparable susceptibility to T-20.   These results indicate that sequence variations in the V3 region do not always correlate with the observed T-20 susceptibility and are not involved in the resistance to C34 and its derivatives.

3.2. Amino acid sequence.

Amino acid sequences of clinical isolates are shown in **Fig. 2b**.   One isolate, HIV-1$_{KT}$, was obtained from a drug naïve patient and the other three isolates (HIV-1$_{411}$, HIV-1$_{412}$, HIV-1$_{A03}$) were obtained from heavily drug-experienced patients.   None of the patients had received T-20 therapy.   Amino acid sequences of the N-HR were highly conserved within all HIV-1 clinical isolates with some small variations.   In contrast, the N36 region of the two HIV-2 strains, EHO and ROD, was identical in both HIV-2 isolates.   We found some variations

12

in the amino acid sequences of the HIV-2 strains we isolated, as compared with the sequences

deposited in the GenBank (accession number; M15390 and X05291 for HIV-2$_{ROD}$, and U272000

for HIV-2$_{EHO}$). Namely, we identified two different amino acids in the isolated HIV-2$_{ROD}$,

V26L and I157I/M (mixture of I and M), and one variation in the amino acid sequence of

HIV-2$_{EHO}$, V45L. Except for I157M, other substitutions are observed in the majority of the

HIV-2 strains, as reported in the HIV sequence database (Los Alamos National Laboratory: Los

Alamos, NM, USA, http://www.hiv.lanl.gov). These substitutions might be introduced through

different culture conditions, (*e.g.,* host cells used for the propagation). We considered these

substitutions as a polymorphism.

Sequence homology of the N36 region of the isolated HIV-1 strains was 31/36 (86%),

including mutation D36G that is observed in the vast majority of HIV-1 strains (Kuiken, et al

2001). In contrast, those of the C34 region were relatively heterogeneous, 24/34 (71%) for

HIV-1 and 12/34 (35%) for HIV-2. Sequence identity of the T-20 region (residues 117-152) in

the HIV-1 strains was also variable 27/36 (75%), while in the HIV-2 strains the sequence

identity was 15/36 (42%). These results indicate that even highly conserved two helical

extracellular domain of the gp41 can allow polymorphisms.

3.3. Efficacy of the peptides against clinical isolates

To evaluate preclinical efficacy, we examined the antiviral activity of C34, SC34 and

SC34EK against clinical isolates (**Table 2**). Replication of HIV-1$_{NL4-3}$ and HIV-1$_{KT}$, a drug

naïve strain, was suppressed by all compounds tested. C34 showed decreased activity against

HIV-1$_{IVR-A03}$, which was isolated from a heavily drug-exposed patient.   SC34 also showed

reduced susceptibility against three drug-experienced strains.   However, it is difficult to

conclude whether SC34 showed enhanced susceptibility against HIV-1$_{KT}$ or reduced

susceptibility against drug resistant strains.   In contrast, T-20 and SC34EK suppressed the

replication of all isolates tested to similar extents in EC$_{50}$ values compared to HIV-1$_{NL4-3}$ (**Table**

2), indicating that SC34EK with appropriately aligned EK residues effectively suppresses the

replication of the clinical isolates.

3.4. Anti-HIV-2 activity

To confirm the target specificity, we examined antiviral activities of SC34 and SC34EK

against two HIV-2 strains, EHO and ROD.   Compared to HIV-1$_{NL4-3}$, EHO and ROD contain

19 and 22 amino acid substitutions in the C34 region, respectively, and 15 amino acid

substitutions in the N36 region, the anticipated site of binding of SC34 and SC34EK peptides

(**Fig. 2b**).   Like the parent peptide C34, both SC34 and SC34EK lost their potent activities

(**Table 3**).   Compared to HIV-1 $_{NL4-3}$, 6 out of 19 residues in the C34 region of HIV-2$_{EHO}$ and 7

out of 22 residues in the C34 region of HIV-2$_{ROD}$ are located at positions *a*, *d*, and *e* that directly

interact with the N36 binding surface.   These substitutions in the N36 and C34 region in HIV-2

may be responsible for reduced anti-HIV-2 activities of the peptides derived from HIV-1.   At

present, we cannot conclude which amino acid substitutions are directly involved in the reduced

susceptibility of the HIV-2 strain to the treatment with the peptide fusion inhibitor, and/or

whether other regions besides the N36 and C34 regions might influence peptide susceptibility.

However, our results indicate that SC34 and SC34EK maintain similar target specificity to the parent peptide, C34.

3.5. Effect of fetal calf serum (FCS) on anti-HIV-1 activity

To estimate the stability of the peptides in vivo, binding level of SC34EK, to serum components, (e.g., albumin) was examined. In this experiment, the antiviral activity in the presence of relatively high concentrations of fetal calf serum (FCS) was determined (Baba et al., 1993) (**Fig. 3**). EC_{80} values of the fusion inhibitors against HIV-1 replication in vitro were used. In the presence of 50% FCS, the activity of MKC-442 (I-EBU), a lipophilic non-nucleoside RT inhibitor, was reduced 2.3-fold compared with 10% FCS as described previously (Baba et al., 1993). However, the activities of SC34, SC34EK and T-20 were little influenced by serum components. Among the three, SC34EK was the least affected by the concentration of FCS.

We further examined the stability of peptide inhibitors in freshly prepared human sera (n = 3). After 1 h incubation of peptides in human sera (final concentration of 200 μM) at 37°C, the anti-HIV-1 activity was examined using the MAGI assay. Comparable activities of all peptides tested were observed either with or without the incubation (data not shown). These results indicate that hydrophilic SC34EK likely retains its strong anti-HIV-1 activity in vivo, similarly to T-20, because of its low nonspecific binding and protease cleavage in serum.

3.5. Peptide binding affinity

To clarify the mechanism of potent anti-HIV-1 activity observed with SC34EK, the

binding affinity of SC34EK was evaluated by collecting the CD spectra using synthetic peptides.

The CD spectra of equimolar mixtures of the N- and C-HR peptides showed spectrum minima

at 208 and 222 nm, which indicate the presence of stable α-helical conformations.   All

combinations of peptides showed similar spectra at 25ºC, indicating that these peptides

contained the same α-helicity (**Fig. 4a**), although the spectrum of C34 with N36 and N43D

mutation (N36$_{N43D}$) indicated only weak α-helicity.   These results indicate that N43D might

reduce the stability of the conformation of the 6-helix bundle, thus decreasing the replication of

HIV-1, whereas V38A does not.   SC34EK formed stable 6-helix conformations with N36$_{V38A}$

and N36$_{N43D}$.   Under these experimental conditions, wavelength-dependent spectra were

similar with the exception of the spectrum of the N36$_{N43D}$/C34 complex.   Thus, we analyzed

thermal stabilities, defined as the midpoint of the thermal unfolding transition (T_m) values, of the

potential 6-helix bundles of N- and C-HR peptides. T_m of N36/C34 was found to be 52.0ºC,

while that of N36$_{V38A}$/C34 and N36$_{N43D}$/C34 decreased to 44.5 and 34.0 ºC, respectively (**Fig.**

3B).   In contrast, thermal stabilities of N36$_{V38A}$/SC34EK, N36$_{N43D}$/SC34EK and N36/SC34EK

were much higher, 60.5, 56.0 and 69.5ºC, respectively.   Thus, binding affinity of SC34EK to

N-HR was stronger compared to that of C34.   Alternatively, at the physiological temperature of

37ºC, only 60 and 40% of the α-helix content was observed in N36$_{V38A}$/C34 and N36$_{N43D}$/C34

mixtures, respectively, indicating that roughly half of C34 failed to form stably 6-helix bundle

with the target N-HR harboring resistant mutations.   Therefore, C34 reduces its anti-fusion

activity exerted by dominant negative effect.   In contrast, only 20% of the unfolded α-helix

content was observed in SC34EK with mutated N36, which indicated that at 37ºC, binding of

SC34EK to mutated N36 was comparable to that of C34 with wild-type N36 (**Fig. 4b**).

Moreover, physiochemical properties of N-HR and SC34EK complexes, defined by T_m value,

correlated well with their ability to inhibit HIV-1 fusion (**Fig. 4c**).   These results suggest that

the stability of the 6-helix complex, as judged by the binding stability (affinity), is directly

correlated with the anti-HIV-1 activity.

3.6. Crystal structure of the N36/SC34EK complex

The crystal structure of the complex between SC34EK and the N-HR representative

peptide N36 was resolved to a resolution of 2.1 Å (**Table 4**).   In the asymmetric unit, a 6-helix

bundle consisting of a central helix bundle of three N36 peptides surrounded by three SC34EK

peptides was found.   This arrangement is similar in the core structure of gp41 (Chan et al.,

1997).   Structural superimposition of the original gp41 core and the N36/SC34EK complex

showed a good match, with an RMSD value of 0.59 for main-chain atoms (**Fig. 5a and b**).

Hydrophobic contacts between SC34EK and N36 with tryptophan rich domain (WRD) and

leucine zipper were preserved for the original gp41 core.   All introduced charged residues of

the EK motif were directed toward the solvent (**Fig. 5c**).   As a direct consequence of

introducing the EK motifs, the ratio of surface area occupied by charged residues to the total

surface area was increased from 35% in the original molecule to 60% in the N36/SC34EK

complex.   Importantly, it appeared that tight bonding, such as ion pairing or hydrogen bonding,

was not present in the side-chains of the residues of the EK motif.   Electrostatic interaction

may involve in constrained structure which provides the enhanced α-helicity observed (**Fig. 4**).

This structural analysis demonstrated that the interaction between N36 and SC34EK retained

the ability to form the 6-helix bundle structure despite the substitution of more than one third of

the residues (13/34) in the sequence of SC34EK.

4. Discussion

In this study, we characterized a novel α-helical peptide, SC34EK that effectively inhibits

replication of HIV-1 strains resistant to T-20 and C34.   The activity was specific to HIV-1 and

little influenced by serum components. We demonstrate that the potent anti-HIV-1 activity of

SC34EK is derived from its high affinity to the N-HR region by the CD analysis.   Further, we

reveal that SC34EK binds to its target, N-HR in identical manner that C34 does by the structure

analysis.

The structural analysis of the N36/SC34EK complex clearly demonstrated that the

interaction between SC34EK and N36 peptides was maintained by hydrophobic contacts and

that the EK motif was directed toward the solvent.   The introduction of the EK residues

increased the proportion of accessible surface area occupied by charged residues.   Although

tight bonding was not observed, a continuous electrostatic potential between the EK residues

may serve to stabilize the helix bundle.   Such helix stabilization, which might occur on the

surface of the HIV-1 virion between SC34EK and the N36 region of gp41, could result in the

high anti-HIV-1 activity.   In this regard, SC34EK, containing an aligned EK motif, showed

more potent anti-HIV-1 activity compared to SC34, which has one misaligned EK motif (**Fig. 2a**).   Increasing the hydrophilic surface area may prevent aggregation of SC34EK as compared to parental peptide C34.   Therefore, SC34EK might distribute into the various organs in the body without being trapped and destroyed in the reticular systems or having its activity reduced by non-specific binding to proteins (e.g., albumin) (**Fig. 3**).

We further demonstrate that SC34EK specifically binds to the target, N-HR of HIV-1, since it exerted less activity to two HIV-2 strains that contain 15 amino acid substitutions in the N-HRs compared to HIV-1 NL4-3 strain (**Table 3 and Fig. 2b**).   These results suggest that to develop resistance to SC34EK, at least, certain mutations in not only the N-HR but also the C-HR are required to be introduced.   This might delay emergence of resistant HIV-1 variants to SC34EK in vivo.

So far, some approaches for stabilizing α-helix structures through the introduction of artificial amino acids were reported for HIV-1 fusion inhibitors T-20 (Judice et al., 1997) and C34 (Sia et al., 2002), including an example of an amino acid containing terminal olefin-derived side chains, designed as a substrate for the ring-closing olefin metathesis (Blackwell et al., 2001) and an example of a hydrocarbon-stapled peptides (Phelan et al., 1997)   Walensky et al. applied a hydrocarbon-stapled modification to generate peptides that bind to the BH3 helical domain of Bcl-2, an anti-apoptotic protein, and demonstrated that a synthesized peptide mimic that binds to the BH3 domain activates apoptosis in leukemic cells (Walensky et al., 2004). However, all peptides exerted only moderate activity in vivo, although they showed efficient

binding to the target proteins in vitro (Blackwell et al., 2001; Judice et al., 1997; Sia et al., 2002; Walensky et al., 2004).   It is likely that during the formation of the 6-helix bundle and the fusion process, gp41 changes its conformation drastically, suggesting that a flexible conformation of the peptide may be required to preserve actual inhibition.   Compared with tethered, constrained peptides, EK modification that facilitates electrostatic stabilization displays such flexibility while exhibiting enhanced α-helicity.   Most recently, T290676, a 38 amino acid peptide, has been reported to suppress various fusion inhibitor-resistant strains of HIV-1 (Dwyer et al., 2007).   Like SC34EK, T290676 is substituted with the charged and hydrophilic amino acids, glutamic acid (E) and arginine (R), at the solvent accessible site and shows potent anti-HIV-1 activity.

In conclusion, we have demonstrated that SC34EK selectively inhibits various HIV-1 strains, including T-20 resistant clones, through increased stability of the α-helix.   The sequence of the solvent accessible site of α-helical peptides is replaceable and modifications of this sequence can regulate α-helicity with target specificity.   Therefore, our approach of introducing the EK motif in the α-helical structure of the peptide inhibitor will help to generate future peptide inhibitors with high anti-HIV efficacy and potentially fewer adverse effects.

20

REFERENCES

Aquaro, S., D'Arrigo, R., Svicher, V., Perri, G.D., Caputo, S.L., Visco-Comandini, U., Santoro, M., Bertoli, A., Mazzotta, F., Bonora, S., Tozzi, V., Bellagamba, R., Zaccarelli, M., Narciso, P., Antinori, A. and Perno, C.F. (2006) Specific mutations in HIV-1 gp41 are associated with immunological success in HIV-1-infected patients receiving enfuvirtide treatment. J Antimicrob Chemother 58, 714-22.

Armand-Ugon, M., Gutierrez, A., Clotet, B. and Este, J.A. (2003) HIV-1 resistance to the gp41-dependent fusion inhibitor C-34. Antiviral Res 59, 137-42.

Baba, M., Yuasa, S., Niwa, T., Yamamoto, M., Yabuuchi, S., Takashima, H., Ubasawa, M., Tanaka, H., Miyasaka, T., Walker, R.T. and et al. (1993) Effect of human serum on the in vitro anti-HIV-1 activity of 1-[(2-hydroxyethoxy)methyl]-6-(phenylthio)thymine (HEPT) derivatives as related to their lipophilicity and serum protein binding. Biochem Pharmacol 45, 2507-12.

Baldwin, C.E. and Berkhout, B. (2006) Second site escape of a T20-dependent HIV-1 variant by a single amino acid change in the CD4 binding region of the envelope glycoprotein. Retrovirology 3, 84.

Blackwell, H.E., Sadowsky, J.D., Howard, R.J., Sampson, J.N., Chao, J.A., Steinmetz, W.E., O'Leary, D.J. and Grubbs, R.H. (2001) Ring-closing metathesis of

olefinic peptides: design, synthesis, and structural characterization of

macrocyclic helical peptides. J Org Chem 66, 5291-302.

Cabrera, C., Marfil, S., Garcia, E., Martinez-Picado, J., Bonjoch, A., Bofill, M.,

Moreno, S., Ribera, E., Domingo, P., Clotet, B. and Ruiz, L. (2006) Genetic

evolution of gp41 reveals a highly exclusive relationship between codons 36,

38 and 43 in gp41 under long-term enfuvirtide-containing salvage regimen.

AIDS 20, 2075-80.

Chan, D.C., Chutkowski, C.T. and Kim, P.S. (1998) Evidence that a prominent cavity

in the coiled coil of HIV type 1 gp41 is an attractive drug target. Proc Natl

Acad Sci U S A 95, 15613-7.

Chan, D.C., Fass, D., Berger, J.M. and Kim, P.S. (1997) Core structure of gp41 from

the HIV envelope glycoprotein. Cell 89, 263-73.

Chan, D.C. and Kim, P.S. (1998) HIV entry and its inhibition. Cell 93, 681-4.

Derdeyn, C.A., Decker, J.M., Sfakianos, J.N., Wu, X., O'Brien, W.A., Ratner, L.,

Kappes, J.C., Shaw, G.M. and Hunter, E. (2000) Sensitivity of human

immunodeficiency virus type 1 to the fusion inhibitor T-20 is modulated by

coreceptor specificity defined by the V3 loop of gp120. J Virol 74, 8358-67.

Derdeyn, C.A., Decker, J.M., Sfakianos, J.N., Zhang, Z., O'Brien, W.A., Ratner, L.,

Shaw, G.M. and Hunter, E. (2001) Sensitivity of human immunodeficiency

virus type 1 to fusion inhibitors targeted to the gp41 first heptad repeat involves

distinct regions of gp41 and is consistently modulated by gp120 interactions with the coreceptor. J Virol 75, 8605-14.

Dwyer, J.J., Wilson, K.L., Davison, D.K., Freel, S.A., Seedorff, J.E., Wring, S.A., Tvermoes, N.A., Matthews, T.J., Greenberg, M.L. and Delmedico, M.K. (2007) Design of helical, oligomeric HIV-1 fusion inhibitor peptides with potent activity against enfuvirtide-resistant virus. Proc Natl Acad Sci U S A. 104, 12772-12777.

Ferrer, M., Kapoor, T.M., Strassmaier, T., Weissenhorn, W., Skehel, J.J., Oprian, D., Schreiber, S.L., Wiley, D.C. and Harrison, S.C. (1999) Selection of gp41-mediated HIV-1 cell entry inhibitors from biased combinatorial libraries of non-natural binding elements. Nat Struct Biol 6, 953-60.

Fikkert, V., Cherepanov, P., Van Laethem, K., Hantson, A., Van Remoortel, B., Pannecouque, C., De Clercq, E., Debyser, Z., Vandamme, A.M. and Witvrouw, M. (2002) env Chimeric Virus Technology for Evaluating Human Immunodeficiency Virus Susceptibility to Entry Inhibitors. Antimicrob Agents Chemother 46, 3954-62.

Foda, M., Harada, S. and Maeda, Y. (2001) Role of V3 independent domains on a dualtropic human immunodeficiency virus type 1 (HIV-1) envelope gp120 in CCR5 coreceptor utilization and viral infectivity. Microbiol Immunol 45, 521-30.

Judice, J.K., Tom, J.Y., Huang, W., Wrin, T., Vennari, J., Petropoulos, C.J. and

McDowell, R.S. (1997) Inhibition of HIV type 1 infectivity by constrained

alpha-helical peptides: implications for the viral fusion mechanism. Proc Natl

Acad Sci U S A 94, 13426-30.

Kajiwara, K., Kodama, E. and Matsuoka, M. (2006) A novel colorimetric assay for

CXCR4 and CCR5 tropic human immunodeficiency viruses. Antivir Chem

Chemother 17, 215-23.

Kimpton, J. and Emerman, M. (1992) Detection of replication-competent and

pseudotyped human immunodeficiency virus with a sensitive cell line on the

basis of activation of an integrated beta-galactosidase gene. J Virol 66, 2232-9.

Kodama, E.I., Kohgo, S., Kitano, K., Machida, H., Gatanaga, H., Shigeta, S.,

Matsuoka, M., Ohrui, H. and Mitsuya, H. (2001) 4'-Ethynyl nucleoside

analogs: potent inhibitors of multidrug-resistant human immunodeficiency

virus variants in vitro. Antimicrob Agents Chemother 45, 1539-46.

Kuiken, C., Foly, B., Hahn, B., Marx, P., McCutchan, F., Mellors, J., Wolinsky, S.,

Korber, B. (2001) HIV Sequence Compendium 2001, edited by Kuiken, C.,

Foly, B., Hahn, B., Marx, P., McCutchan, F., Mellors, J., Wolinsky, S., Korber,

B. Los Alamos National Laboratory, Los Alamos, NM.

Lalezari, J.P., Henry, K., O'Hearn, M., Montaner, J.S., Piliero, P.J., Trottier, B.,

Walmsley, S., Cohen, C., Kuritzkes, D.R., Eron, J.J., Jr., Chung, J., DeMasi, R.,

Donatacci, L., Drobnes, C., Delehanty, J. and Salgo, M. (2003) Enfuvirtide, an HIV-1 fusion inhibitor, for drug-resistant HIV infection in North and South America. N Engl J Med 348, 2175-85.

Lazzarin, A., Clotet, B., Cooper, D., Reynes, J., Arasteh, K., Nelson, M., Katlama, C., Stellbrink, H.J., Delfraissy, J.F., Lange, J., Huson, L., DeMasi, R., Wat, C., Delehanty, J., Drobnes, C. and Salgo, M. (2003) Efficacy of enfuvirtide in patients infected with drug-resistant HIV-1 in Europe and Australia. N Engl J Med 348, 2186-95.

Liu, S., Lu, H., Niu, J., Xu, Y., Wu, S. and Jiang, S. (2005) Different from the HIV Fusion Inhibitor C34, the Anti-HIV Drug Fuzeon (T-20) Inhibits HIV-1 Entry by Targeting Multiple Sites in gp41 and gp120. J Biol Chem 280, 11259-73.

Maeda, Y., Foda, M., Matsushita, S. and Harada, S. (2000) Involvement of both the V2 and V3 regions of the CCR5-tropic human immunodeficiency virus type 1 envelope in reduced sensitivity to macrophage inflammatory protein 1alpha. J Virol 74, 1787-93.

Maeda, Y., Venzon, D.J. and Mitsuya, H. (1998) Altered drug sensitivity, fitness, and evolution of human immunodeficiency virus type 1 with pol gene mutations conferring multi-dideoxynucleoside resistance. J Infect Dis 177, 1207-13.

Marqusee, S. and Baldwin, R.L. (1987) Helix stabilization by Glu-.Lys+ salt bridges in short peptides of de novo design. Proc Natl Acad Sci U S A 84, 8898-902.

Matthews, T., Salgo, M., Greenberg, M., Chung, J., DeMasi, R. and Bolognesi, D. (2004) Enfuvirtide: the first therapy to inhibit the entry of HIV-1 into host CD4 lymphocyte. Nature Reviews Drug Discovery 3, 215-225.

McRee, D.E. (1999) XtalView/Xfit--A versatile program for manipulating atomic coordinates and electron density. J. Struct. Biol. 125, 156-165.

Menzo, S., Castagna, A., Monachetti, A., Hasson, H., Danise, A., Carini, E., Bagnarelli, P., Lazzarin, A. and Clementi, M. (2004) Genotype and phenotype patterns of human immunodeficiency virus type 1 resistance to enfuvirtide during long-term treatment. Antimicrob Agents Chemother 48, 3253-9.

Mink, M., Mosier, S.M., Janumpalli, S., Davison, D., Jin, L., Melby, T., Sista, P., Erickson, J., Lambert, D., Stanfield-Oakley, S.A., Salgo, M., Cammack, N., Matthews, T. and Greenberg, M.L. (2005) Impact of human immunodeficiency virus type 1 gp41 amino acid substitutions selected during enfuvirtide treatment on gp41 binding and antiviral potency of enfuvirtide in vitro. J Virol 79, 12447-54.

Murshudov, G.N., Vagin, A.A., Lebedev, A., Wilson, K.S. and Dodson, E.J. (1999) Efficient anisotropic refinement of macromolecular structures using FFT. Acta Crystallogr. D55, 247-255.

Nameki, D., Kodama, E., Ikeuchi, M., Mabuchi, N., Otaka, A., Tamamura, H., Ohno, M., Fujii, N. and Matsuoka, M. (2005) Mutations conferring resistance to

human immunodeficiency virus type 1 fusion inhibitors are restricted by gp41

and Rev-responsive element functions. J Virol 79, 764-70.

Navaza, J. (2001) Implementation of molecular replacement in AMoRe. Acta

Crystallogr. D57(Pt 10), 1367-1372.

Otaka, A., Nakamura, M., Nameki, D., Kodama, E., Uchiyama, S., Nakamura, S.,

Nakano, H., Tamamura, H., Kobayashi, Y., Matsuoka, M. and Fujii, N. (2002)

Remodeling of gp41-C34 peptide leads to highly effective inhibitors of the

fusion of HIV-1 with target cells. Angew Chem Int Ed Engl 41, 2937-40.

Otwinowski, Z. and Minor, W. (1997) Processing of X-ray diffraction data collected in

oscillation mode. Met. Enzymol. 276, 307-326.

Phelan, J.C., Skelton, N.J., Braisted, A.C. and McDowell, R.S. (1997) A General

Method for Constraining Short Peptides to an Alpha-Helical Conformation. J

Am Chem Soc 119, 455-460.

Poveda, E., Rodes, B., Labernardiere, J.L., Benito, J.M., Toro, C., Gonzalez-Lahoz, J.,

Faudon, J.L., Clavel, F., Schapiro, J. and Soriano, V. (2004) Evolution of

genotypic and phenotypic resistance to Enfuvirtide in HIV-infected patients

experiencing prolonged virologic failure. J Med Virol 74, 21-8.

Poveda, E., Rodes, B., Toro, C., Martin-Carbonero, L., Gonzalez-Lahoz, J. and Soriano,

V. (2002) Evolution of the gp41 env region in HIV-infected patients receiving

T-20, a fusion inhibitor. AIDS 16, 1959-61.

Reeves, J.D., Gallo, S.A., Ahmad, N., Miamidian, J.L., Harvey, P.E., Sharron, M.,

Pohlmann, S., Sfakianos, J.N., Derdeyn, C.A., Blumenthal, R., Hunter, E. and

Doms, R.W. (2002) Sensitivity of HIV-1 to entry inhibitors correlates with

envelope/coreceptor affinity, receptor density, and fusion kinetics. Proc Natl

Acad Sci U S A 99, 16249-54.

Rimsky, L.T., Shugars, D.C. and Matthews, T.J. (1998) Determinants of human

immunodeficiency virus type 1 resistance to gp41-derived inhibitory peptides. J

Virol 72, 986-93.

Salzwedel, K., West, J.T. and Hunter, E. (1999) A conserved tryptophan-rich motif in

the membrane-proximal region of the human immunodeficiency virus type 1

gp41 ectodomain is important for Env-mediated fusion and virus infectivity. J

Virol 73, 2469-80.

Sia, S.K., Carr, P.A., Cochran, A.G., Malashkevich, V.N. and Kim, P.S. (2002) Short

constrained peptides that inhibit HIV-1 entry. Proc Natl Acad Sci U S A 99,

14664-9.

Walensky, L.D., Kung, A.L., Escher, I., Malia, T.J., Barbuto, S., Wright, R.D., Wagner,

G., Verdine, G.L. and Korsmeyer, S.J. (2004) Activation of apoptosis in vivo by

a hydrocarbon-stapled BH3 helix. Science 305, 1466-70.

Wei, X., Decker, J.M., Liu, H., Zhang, Z., Arani, R.B., Kilby, J.M., Saag, M.S., Wu, X.,

Shaw, G.M. and Kappes, J.C. (2002) Emergence of resistant human

immunodeficiency virus type 1 in patients receiving fusion inhibitor (T-20) monotherapy. Antimicrob Agents Chemother 46, 1896-905.

Weiner, M.P., Costa, G.L., Schoettlin, W., Cline, J., Mathur, E. and Bauer, J.C. (1994) Site-directed mutagenesis of double-stranded DNA by the polymerase chain reaction. Gene 151, 119-23.

Wild, C., Oas, T., McDanal, C., Bolognesi, D. and Matthews, T. (1992) A synthetic peptide inhibitor of human immunodeficiency virus replication: correlation between solution structure and viral inhibition. Proc Natl Acad Sci U S A 89, 10537-41.

Xu, L., Pozniak, A., Wildfire, A., Stanfield-Oakley, S.A., Mosier, S.M., Ratcliffe, D., Workman, J., Joall, A., Myers, R., Smit, E., Cane, P.A., Greenberg, M.L. and Pillay, D. (2005) Emergence and evolution of enfuvirtide resistance following long-term therapy involves heptad repeat 2 mutations within gp41. Antimicrob Agents Chemother 49, 1113-9.

Xu, Y., Hixon, M.S., Dawson, P.E. and Janda, K.D. (2007) Development of a FRET assay for monitoring of HIV gp41 core disruption. J Org Chem 72, 6700-7.

FIGURE captions

Fig. 1. Helical wheel representation of the 6-helix bundle structure and the design of

SC34EK. (a) Amino acid residues at positions *a, d, e* of C34 are interactive sites that form

the 6-helix complex with N36, while the remaining amino acid residues at positions *b, c, f, g*

are solvent accessible sites, which are substituted with Glu (E) or Lys (K) in SC34EK. **(b)**

The design concept of introducing the EK motif to the solvent accessible site. The α-helical

C-HR peptide could be divided into interactive (red) and solvent (blue) sites. Z indicates the

original amino acids of C34. Only amino acid residues at solvent sites were replaced by E at

the *i* position and K at the i+4 position.

Fig. 2. Schematic view of gp41 and C34 derivatives and amino acid alignment of gp41.

(a) The locations of the fusion peptide (FP), the amino-terminal heptad repeat region (N-HR),

the carboxyl-terminal heptad repeat region (C-HR), and the transmembrane domain (TM) and

the amino acid sequences of N36, T-20, C34 and its derivatives are shown. The residue

numbers of each peptide correspond to their positions in gp41 of the NL4-3 strain. The X in

SC34EK indicates norleucine, introduced to avoid oxidation of the methionine residues. No

differences between the original methionine- and norleucine-containing peptide were observed

(Otaka et al., 2002). **(b)** Alignment of amino acid sequence of clinical isolates (KT, IVR411,

IVR412 and IVR-A03; GenBank accession number; **AB222704**, **AB222705**, **AB222706** and

AB222703, respectively) and HIV-2 strains (EHO and ROD) are shown. Corresponding

regions of N36 and C34 are indicated in gray.   Identical or deleted amino acids from the

sequence of NL4-3 are indicated with a bar or a dot, respectively.   The X in amino acid

sequences of IVR411 and ROD indicates the mixture of I and V for IVR411, and mixture of I

and M for ROD.

Fig. 3.   Effect of FCS concentrations on anti-HIV-1 activity.   Changes in the blue cell

counts at various concentrations of FCS are shown.   Blue cell counts at EC_{80} value in 10%

FCS concentration (black bar) were used and set as 100%．   White, black, hatched, and striped

bars correspond to 5, 10, 25, and 50% FCS, respectively.   Inhibitors for reverse transcriptase,

ddC and MKC-442, and for fusion, T-20 were used as controls.

**Fig. 4.   CD analysis of peptide complex between resistant variants of N36 and C34 or

SC34EK.**   **(a)** Wavelength-dependent CD spectra of the complexes in solution.   The

spectrum minima at 208 and 222 nm indicated the presence of stable α-helical conformations.

(b) Thermal midpoint analysis was measured at 222 nm CD signal for the N and C peptide

complexes.   Final concentration of each peptide was 10 mM.   The arrow indicates the

physiological temperature of 37ºC.   **(c)** The correlation between T_m (Fig. 3B) and EC_{50} values

(**Table 1**).   Colors of plots correspond to those in panels **(a)** and **(b)**.   Combination of

$N36_{N43D}$ and C34 ($EC_{50} > 100$ nM) is excluded.

Fig. 5. Structure of the 6-helix bundle formed by N36 and SC34EK. (a) and **(b)** The

gp41 core structure and N36/SC34EK complex are shown in red and blue, respectively. **(c)**

Stick model representation of SC34EK.   The stick model of SC34EK is shown, and three

N36s in the core and two other surrounded SC34EK are represented in gray.   SC34EK

showed amphiphilic properties.   The location of the N-terminal tryptophan rich domain

(WRD) in SC34EK is indicated by a red circle.   Original and introduced charged amino acids

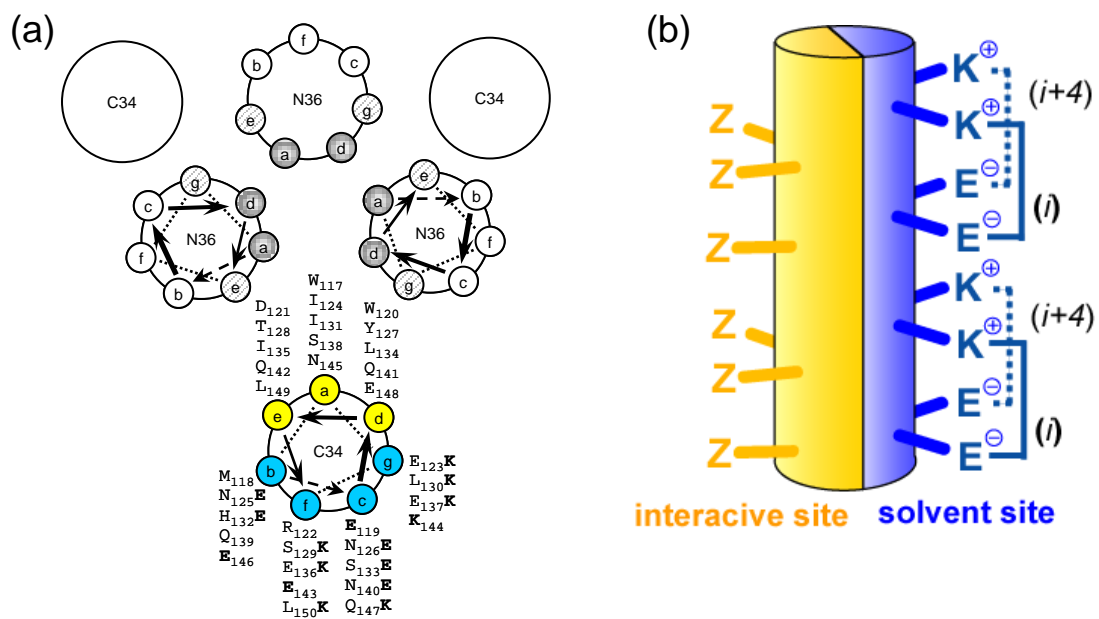are indicated in green and blue, respectively.

Fig. 1.

(a)

(b)

Fig. 2.

(a)

Extracellular ← → Intracellular

NH₂ — FP — HR1 — HR2 — TM — //— COOH

35   70
N36

117   150
C34

```
N36   SDIVQQQNNLLRAIEAQQHLLQLTVWGIKQLQARIL

C34      WMEWDREINNYTSLIHSLIEESQNQQEKNEQELL
SC34     ------K-EE--KK-KK------E------K--K
SC34EK   -Z----K-EE--KK-EE--KK--E------K--K
T-20           YTSLIHSLIEESQNQQEKNEQELLELDKWASLWNWF
```

(b)

```
                                         N36
          1                 36 38  43              70              100
NL4-3   AVGIGALFLGFLGAAGSTMGAASMTLTVQARQLLSDIVQQQNNLLRAIEAQQHLLQLTVWGIKQLQARILAVERYLKDQQLLGIWGCSGKLICTTAVPWN
IVR-KT  --TL--V---------------L-------L--G-----------------M------------V-------------------------T----
IVR-411 ----------------------I----------G-----------------------------X----------------------------------
IVR-412 --TF------------------I----------G-----------------------------R--------------------------T----
IVR-A03 -A•L--M--------------I----H-----YG----------K-----------G--R---------R-----S----

EHO     G-•LVLG-----AT---A-----L--SA-S-T--AG-----QQ--DVVKR--E--R-----T-N----VT-I-K-----AQ-NS---AFRQV-H-T---V
ROD     G-•FVLG-----AT---A-----L--SA-S-T--AG-----QQ--DVVKR--E--R-----T-N----VT-I-K---Q--AR-NS---AFRQV-H-T---V
```

```
                          C34                                            TM
          101        117                     150                          200
NL4-3   ASWSNKSLEQIWNNMTWMEWDREINNYTSLIHSLIEESQNQQEKNEQELLELDKWASLWNWFNITNWLWYIKLFIMIVGGLVGLRIVFAVLSIVNRVRQG
IVR-KT  S------MD---D----Q---------N--YT-----------------------D-SK-----RI--------I----I-----K----
IVR-411 ------QDE-------Q---------N--Y----Q-----------------N-------S------I--------I---I-T---V------
IVR-412 V------Q-E-------Q-EK--D---G--YT--K------------------A-----------D--------QI--------I----I----V-------
IVR-A03 T------MDE-------E---D---N--Y--L-K--I-----------------------S--D----------I---------I---I-T------

EHO     ••••-E--KPD------QQ-E-QVRFLDAN--TK-L--A-I------MY--QK-NQ-DIFS---DF-S-MA--R-GLY--I-I-V---AIYIIQMLA-L-K-
ROD     ••••-D--APD-D----QE-EKQVRYLEAN--SKSL-QA-I------MY--QK-NS-DXFG---DL-S-VK--QYGVL-IVAVIA----IY-VQMLS-L-K-
```

35

Fig. 3.

Fig. 4.

(a)

(b)

37 ºC

(c)

R² = 0.72

◆ N36-C34   ■ N36$_{V38A}$-C34   ▲ N36$_{N43D}$-C34
● N36-SC34EK   — N36$_{V38A}$-SC34EK   ● N36$_{N43D}$-SC34EK

Fig. 5.

(a)

(b)

(c)

WRD

Interactive site   Solvent accessible site

Table 1.   Antiviral activity of gp41-derived peptides against gp41 and gp120 V3 recombinant virus[a].

clone	tropism[b]	EC$_{50}$ (nM)					
		ddC	N36	T-20	C34	SC34	SC34EK
gp41 recombinant virus							
WT[c]		404±196	180±70	35±17	3.2±0.9	1.4±0.7	0.7±0.3
L33S		289±24	39±11	**>1000**	2.9±0.9	1.3±0.1	0.9±0.3
V38A		714±109	407±76	**402±68**	**96±29**	2.0±0.5	1.1±0.6
V38E		291±57	41±14	**>1000**	**492±85**	**37±12**	**4.3±1.3**
N43K		321±8.5	234±63	114±19	**50±9.5**	2.5±0.3	2.7±0.3
N43D		430±42	461±266	**>1000**	**>100**	**9.0±6.6**	1.0±0.8
D36S/V38M		296±88	178±31	42±6.4	7.2±4.0	1.9±0.1	0.8±0.3
V38E/N42S		273±105	227±20	**>1000**	**322±7.5**	**32±3.1**	3.2±1.0
ΔFNSTW/L33S/N43K[d]		276±39	152±31	**>1000**	**248±56**	2.7±0.3	**4.4±0.5**
ΔFNSTW/D36G/I37K/N126K/L204I[d]							
		246±67	547±7.8	**754±174**	**67±21**	4.6±0.9	2.9±0.8
gp120 V3 recombinant virus							
V3-ADA	R5	362±102	360±91	**289±19**	6.8±3.3	0.7±0.4	2.0±0.2
V3-SF162[e]	R5	995±219	383±9.9	19±2.8	7.8±3.5	0.5±0.2	0.5±0.2
V3-CH1[f]	R5X4	649±4.5	**2207±42**	16±1	5.6±0.1	1.3±0.1	0.7±0.1
V3-CH2[g]	R5	1515±177	192±13	35±32	3.8±0.1	0.4±0	0.9±0.8

[a]Anti-HIV-1 activity was determined using the MAGI assay.   All data represent means ± standard deviation obtained from the results of three independent experiments.   Bold indicates over 5-fold increase in EC$_{50}$ value compared to HIV-1$_{WT}$.   [b]The co-receptor tropism were determined using NCK45 cells as described (Kajiwara et al., 2006).   [c]HIV-1$_{NL4-3}$ served as a wild-type virus.   [d]ΔFNSTW is the deletion of five amino acids at position 364-368 in the gp120 V4 region of HIV-1$_{NL4-3}$ (Nameki et al., 2005).   Fusion inhibitor resistant variants used have been previously reported (Armand-Ugon et al., 2003; Nameki et al., 2005).   [e]The V3 region of NL4-3 gp120 was replaced with the corresponding region of HIV-1$_{SF162}$.   [f]HIV-1$_{V3-CH1}$ has mutations in the gp120 V3 region of primary isolate HIV-1$_{KMT}$, where GKI is substituted by GEI.   [g]HIV-1$_{V3-CH2}$ has mutation in the gp120 V3 region of the primary isolate HIV-1$_{KMT}$, where GKI is substituted by GQI.

Table 2. **Antiviral activity of gp41-derived peptides against clinical isolates[a].**

Strain	EC$_{50}$ (nM)				
	AZT	T-20	C34	SC34	SC34EK
NL4-3 (WT)[b]	2.0	36	3.2	0.36	0.4
KT (WT)[b]	2.0	11	0.2	0.1	0.03
IVR411	**7600**	4.1	0.2	3.1	0.04
IVR412	**9060**	23	7.2	**4.8**	0.1
IVRA03	**1200**	7.0	**17**	**4.1**	0.7

[a]Anti-HIV-1 activity was determined using the amounts of p24 protein in the supernatants of the PHA-stimulated PBMC cultures using commercially available ELISA kit (Kodama et al., 2001).   Bold indicates over 5-fold increase in EC$_{50}$ value compared to HIV-1$_{WT}$.   [b]HIV-1$_{NL4-3}$ and HIV-1$_{KT}$ served as controls.

Table 3. Antiviral activity of HIV-1 gp41-derived peptides against HIV-2[a].

HIV-2 strain	EC$_{50}$ (nM)				
	ddC	T-20	C34	SC34	SC34EK
WT[b]	404±196	35±17	3.2±0.9	1.4±0.7	0.7±0.3
HIV-2$_{EHO}$[c]	925±188	14±3.0 (x0.4)	**639±87 (x200)**	**68±10 (x49)**	**17±1.2 (x24)**
HIV-2$_{ROD}$[d]	**1,808±927**	**176±68 (x5)**	**>1000 (> x313)**	**251±29 (x179)**	**115±33(x164)**

[a]Anti-HIV-2 activity was determined using the MAGI assay.   All data represent mean ± standard deviation obtained from the results of three independent experiments.   Bold indicates over 5-fold increase in EC$_{50}$ value compared to HIV-1$_{WT}$.   [b]HIV-1$_{NL4-3}$ served as a wild-type virus.   [c]HIV-2$_{EHO}$ was dual-tropic HIV-2. [d]HIV-2$_{ROD}$ was T-tropic HIV-2.

Table 4. Crystallization, data collection and refinement statistics.

Data collection	BL38B1 Spring-8
Temperature (K)	100
Space group	$P3_121$
Cell dimensions a, b, c (Å)	105.01, 105.01, 78.31
Resolution limits (Å)	90.00 - 2.10
No. unique reflections	29,461
Average redundancy	7.53
Completeness (%)	99.7
R_{merge} [a]	0.122
Refinement statistics	
Refinements resolution range (Å)	20.00 - 2.20
R / R_{free} [b] (%)	0.213/0.238
The highest resolution shell (Å)	2.15 – 2.10
R / R_{free} [b] (%)	0.231/0.255
RMSD from ideal	
bonds (Å)	0.010
angles (°)	1.015
$<B>$ for atomic model [c] (Å^2)	29.93
Ramachandran plot	
Most favored regions (%)	100

[a] $R_{merge} = \Sigma| I_h - <I_h>| / \Sigma I_h$, where $<I_h>$ is the average intensity of reflection h and symmetry-related reflections. [b] R and $R_{free} = \Sigma||F_o|-|F_c||/\Sigma|F_o|$ calculated for reflections of the working set and test (5%) set, respectively. [c] $<B>$ is the average temperature factor for all protein atoms.